



**HAL**  
open science

## Global search of non-linear systems periodic solutions: A rotordynamics application

Emmanuelle Sarrouy, Fabrice Thouverez

### ► To cite this version:

Emmanuelle Sarrouy, Fabrice Thouverez. Global search of non-linear systems periodic solutions: A rotordynamics application. *Mechanical Systems and Signal Processing*, 2010, 24 (6), pp.1799-1813. 10.1016/j.ymssp.2010.02.001 . hal-00623621

**HAL Id: hal-00623621**

**<https://hal.science/hal-00623621>**

Submitted on 14 Sep 2011

**HAL** is a multi-disciplinary open access archive for the deposit and dissemination of scientific research documents, whether they are published or not. The documents may come from teaching and research institutions in France or abroad, or from public or private research centers.

L'archive ouverte pluridisciplinaire **HAL**, est destinée au dépôt et à la diffusion de documents scientifiques de niveau recherche, publiés ou non, émanant des établissements d'enseignement et de recherche français ou étrangers, des laboratoires publics ou privés.

# Global search of non-linear systems periodic solutions: a rotordynamics application

E. Sarrouy<sup>\*,\*\*a,1</sup>, F. Thouverez<sup>a</sup>

<sup>a</sup>*Ecole Centrale de Lyon, Bat. E6, 36 avenue Guy de Collongue, 69134 Ecully Cedex, France*

---

## Abstract

Introducing non-linearities into models contributes towards a better reality description but leads to systems having multiple solutions. It is then legitimate to look for all the solutions of such systems, that is to have a global analysis approach. However no effective method can be found in literature for systems described by more than two or three degrees of freedom. We propose in this paper a way to find all  $T$ -periodic solutions - where  $T$  is known - of a non-linear dynamical system. This method is compared to three other approaches and is shown to be the most efficient on a Duffing oscillator. As a more complex example, a rotor model including a squeeze-film damper is studied and a second branch of solutions is exhibited.

*Key words:* Global analysis, Non-linear, Homotopy, Polynomial, Rotordynamics, Squeeze-film damper

---

## 1. Introduction

Global analysis of dynamical systems is of great interest in industrial development as well as in research area. Introduction of non-linear organs in dynamical modeling is one of the ways to a better reality description and so to a better behavior prediction; though it induces multiple solutions of varied nature (periodic, quasi-periodic...). One need to get them all in order to dimension a structure properly. Then, when trying to get the solutions of a set of non-linear dynamical equations, two approaches, local or global, are possible. Local methods mostly consist in choosing a startpoint and having many correction steps until a solution point is found. On the contrary, global analysis methods consider the whole state space (or a bounded part of it) and try to find all the solutions contained in it.

Many methods aim at global analysis of non-linear systems of equations. They all share the same problem: their computational efficiency. In this paper a new approach is proposed for locating all  $T$ -periodic solutions. It is based on the transformation of the dynamical system into a non-differential one followed by a polynomial approximation of the non-linear part of this equivalent system; then a global resolution of the resulting polynomial system is achieved using a homotopy method. Our approach is compared to three existing methods: simple cell-mapping, a test exclusion based

---

\*Corresponding author

\*\*Tel: +33 681393569/Fax:+33 144246468

*Email addresses:* [emmanuelle.sarrouy@gmail.com](mailto:emmanuelle.sarrouy@gmail.com) (E. Sarrouy), [fabrice.thouverez@ec-lyon.fr](mailto:fabrice.thouverez@ec-lyon.fr) (F. Thouverez)

<sup>1</sup>Present adress: Arts et Metiers ParisTech - CER de Paris, Laboratoire LMSP, 151 boulevard de l'Hôpital, 75013 Paris, France

method and one relying on interval analysis. Section 2.1 presents a short overview and references for each existing method used for comparison while section 2.2 exposes the proposed method in a detailed way.

The four methods are applied to a Duffing oscillator and compared in section 3; this demonstrates efficiency of the suggested approach. Finally, its ability to treat more complex systems and the usefulness of such a global analysis algorithm is illustrated in section 4 through a simplified model of a rotor using a squeeze-film damper.

## 2. Global analysis methods at stake

This part is devoted to the four methods compared in the next section. First, the principles of three existing methods dedicated to global analysis are quickly explained. In a second part, the three main steps of the proposed method are detailed. Among the four treated methods, one (the cell-mapping) treats directly the differential system of equations (1) while the three others require its transformation into a non-linear (non-differential) system of equations (2). In the latter case the same transformation will be used for exclusion test methods, approaches relying on interval analysis and the proposed method. Finding all the T-periodic solutions of (1) or finding all the solutions of (2) is equivalent if a proper transformation is used. A way to do so is exposed in part 2.2.1.

*Ordinary differential equations.*

$$\mathbf{M}\ddot{q} + \mathbf{C}\dot{q} + \mathbf{K}q + \hat{f}(q, \dot{q}) = f_e(t) \quad (1)$$

where  $\mathbf{M}$ ,  $\mathbf{C}$  and  $\mathbf{K}$  are respectively mass, damping and stiffness matrices,  $\hat{f}(q, \dot{q})$  stands for non-linear efforts depending on displacements and velocities and  $f_e(t)$  is the excitation vector.

*Non-linear (non-differential) system.*

$$\mathbf{H}\tilde{x} + \hat{H}(\tilde{x}) = H_e \quad (2)$$

with  $\tilde{x}$  containing generalized unknowns,  $\mathbf{H}$  denoting the linear part of equation,  $\hat{H}(\tilde{x})$  its non-linear part and  $H_e$  its constant term.

### 2.1. Existing methods overview

First of all is the cell-mapping [10] which consists in discretization of a bounded part of the state space in small “cells” (the rest of the state space is represented by a special “sink cell”) and a short time integration of one or more points of each of these cells. The entire state space evolution along time can then be built and all kinds of solutions and their basins of attraction can be found. For example, let’s consider a non-linear dynamical system of dimension 1 (with dimension 2 state space) and let  $q$  and  $\dot{q}$  denote the displacement and velocity. Figure 1 shows a possible discretization used for the state space portion of interest  $(q, \dot{q}) \in [q_{min}, q_{max}] \times [\dot{q}_{min}, \dot{q}_{max}]$ . The eight cells centers are startpoints for a time integration with duration  $\tau$  (for non-autonomous system,  $\tau$  often refers to excitation period, and to a characteristic time otherwise). The cell which contains the point after time-integration is the image cell of the cell in which time integration started. In figure 1, this mapping is drawn using arrows. On such a simple example,

the analysis would lead to the detection of two cycles: one cycling through cells number 2,7 and 6 and the other one alternating between cells 4 and 5. Basins of attraction of these cycles are respectively cell 1 and cell 3. Cell 8 maps to the sink cell.

[Figure 1 about here.]

The illustrated branch of cell-mapping is the simple cell-mapping; some more elaborated versions can be found in literature ([7, 4]). This method is quite natural because it deals with dynamical equations and seems attractive by finding all kinds of solutions and their basins of attraction, about what no other method can boast. The problem holds in the huge storage resource and computational time required to apply such a method.

*Methods using exclusion tests* require the transformation of (1) into (2). Then, a bounded part  $\Omega$  of  $\mathbb{R}^{\tilde{n}}$  (where  $\tilde{x}$  varies) needs to be defined: that is where the solutions of (2) are sought. The algorithm tries to exclude portions of  $\Omega$  using a cell-discarding-condition (CDC)[26]: if the test is positive the cell contains no solution and is put away; otherwise, the cell is kept and divided in two or more sub-cells that will be tested in turn. Figure 2 shows the general scheme of such methods. Their efficiency depends on both the quality of the test regarding the set of equations under study and its complexity: if it does not manage to eliminate big cells (big parts of  $\Omega$ ) it will fail in investigating the whole space in a reasonable amount of time, so it has to be of good quality but it should not cost too much (i.e. be too much complex) to avoid spending a lot of time when applied to a cell.

[Figure 2 about here.]

The authors chose to use a test based on phase I of the simplex method [27]. This test is easy to implement and does not require any property for the non-linearity  $\hat{H}(\tilde{x})$ . More specific tests can be found in [5, 6].

*Interval analysis based methods* also process systems of form (2) rather than differential systems. As the previous method, they need a bounded part  $\Omega$  of  $\mathbb{R}^{\tilde{n}}$  to be defined. This first cell is then partitioned leading to a collection of cells  $\Gamma$ . The main distinctive feature of these methods is that they no longer deal with real numbers but with intervals: usual operations such as “+”, “-”, etc. are redefined [1]. Such algorithms try both to exclude cells and to reduce them (using other ways than simple splitting). Hansen and Walster [9] propose an interesting algorithm that has two different approaches depending on the current cell size: some routines are dedicated to “big” cells and are cheap in term of computation cost; when a cell is “small” enough and has some properties, some other techniques, more costly are implemented to refine or exclude it. Figure 3 gives a simplified overview of this algorithm.

[Figure 3 about here.]

Main steps are Global approach processing (designed for big cells) and Local approach processing (designed for small cells). As it is a far complex algorithm, we do not give all the details for each main step but we rather give one representative routine for each. Let us denote  $\tilde{X}$  the cell being processed (interval of  $\mathbb{R}^{\tilde{n}}$ ) and  $\tilde{x}$  a point of this cell (in  $\mathbb{R}^{\tilde{n}}$ ).

- Global approach example: the hull consistency test. This method tries to take advantage of the linear part of system (2) which is the easiest part to deal with. Looking for a solution of (2), one can rewrite the equation in the following way

$$\begin{aligned} & \forall i \in \{1, \dots, \tilde{n}\}, \mathbf{H}_{ij}\tilde{X}_j + \hat{H}_i(\tilde{X}) - H_e = 0 \\ \Leftrightarrow & \forall i \in \{1, \dots, \tilde{n}\}, \forall k \in \{1, \dots, \tilde{n}\}, \mathbf{H}_{ik}\tilde{X}_k + \sum_{j \neq k} \mathbf{H}_{ij}\tilde{X}_j + \hat{H}_i(\tilde{X}) - H_e = 0 \end{aligned}$$

with  $\tilde{n}$  denoting  $\tilde{x}$  dimension. It is then obvious that each component interval  $\tilde{X}_k$  can be reduced to its intersection with  $\tilde{X}'_k$  satisfying

$$\mathbf{H}_{ik}\tilde{X}'_k = -\hat{H}_i(\tilde{X}) + H_e \ominus \sum_{j \neq k} \mathbf{H}_{ij}\tilde{X}_j, \quad 1 \leq i \leq \tilde{n}$$

with  $\ominus$  standing for  $X \ominus Y = [\inf X - \sup Y, \sup X - \inf Y]$ . Reusing already reduced  $\tilde{X}_k$  for reduction of  $\tilde{X}_m$ ,  $k < m$ , this technique can lead to a cell exclusion (if  $\tilde{X}_k \cap \tilde{X}'_k$  is empty) or at least to a great reduction using only simple operations.

- Local approach example: the newton like method. When the cell  $\tilde{X}$  is small enough, some expansion around a well chosen point  $\tilde{x}_0 \in \mathbb{R}^{\tilde{n}}$  is a good approximation of non-linear part  $\hat{H}(\tilde{x})$  on the cell. Let's define  $H(\tilde{x}) = \mathbf{H}\tilde{x} + \hat{H}(\tilde{x}) - H_e$ . If  $H$  is regular enough

$$\forall \tilde{x} \in \tilde{X}, \exists \zeta \in \tilde{X}, H(\tilde{x}) = H(\tilde{x}_0) + \mathbf{J}(\zeta)(\tilde{x} - \tilde{x}_0)$$

with  $\mathbf{J}(\tilde{x}) = \left[ \frac{\partial H_i}{\partial \tilde{x}_j}(\tilde{x}) \right]_{ij}$ .

The trick is to replace the unknown  $\zeta$  by the whole cell  $\tilde{X}$ . Then if a solution  $\tilde{x}^*$  exists in the cell  $\tilde{X}$ , one can write

$$0 \in H(\tilde{x}_0) + \mathbf{J}(\tilde{X})(\tilde{x}^* - \tilde{x}_0)$$

This provides a new  $\tilde{X}'$  interval containing all the solutions  $\tilde{x}$  of

$$\mathbf{J}(\tilde{X})(\tilde{x} - \tilde{x}_0) = -H(\tilde{x}_0)$$

which is a Newton like equation. As in the hull consistency test,  $\tilde{X} \cap \tilde{X}'$  may be empty or lead to  $\tilde{X}$  reduction.

Unfortunately, these three global analysis methods appear to be inefficient as soon as the system becomes greater than 2 or 3 degrees of freedom (dofs): if their mathematical background ensures to obtain all the solutions, the numerical resource and the computational time needed to treat the problem explode and most of the time one can predict neither this cost nor this time (see section 3).

## 2.2. Proposed polynomial homotopic method

A polynomial approximation of the non-linear part of system (2) is used in order to save time. Being in a well-defined space of multi-variable polynomial systems helps to apply more efficient methods like homotopies in order to

find all the solutions of the algebraic system. In order to exhibit all  $T$ -periodic solutions of (1), one need to convert it into a non-differential equivalent system (2), then to turn this system into an algebraic one (i.e. a multi-variable polynomial system) and finally to solve this system “globally”. Each of these three steps is detailed in the followings subsections.

### 2.2.1. From differential to non-differential equations

First of all, one needs to convert the dynamical formulation (1) into a non-differential system of form (2). This is done by making assumptions on the nature of the sought solution  $q(t)$  which, in the present case, is expected to be a  $T$ -periodic solution. One insists on the fact that such a step is usually followed by a local resolution algorithm (of Newton-Raphson type) which leads to one solution at most while a global resolution method will here be applied to the new set of equations in order to exhibit all its solutions.

The transformation relies on the harmonic balance method (HBM) [16, 20, 17] which provides non-differential equations using a Galerkin approach. One assumes that  $q(t)$  is well enough described by a truncated Fourier series using  $N_h$  harmonics:

$$q(t) \approx \frac{a_0}{\sqrt{2}} + \sum_{k=1}^{N_h} a_k \cos(k\omega t) + b_k \sin(k\omega t)$$

with  $\omega = 2\pi/T$ . It is straightforward to express  $\dot{q}$  and  $\ddot{q}$  as  $a_0$ ,  $a_k$  and  $b_k$  functions and then to put back their expressions into (1), obtaining a set of  $n$  non-differential but time dependent equations with  $\tilde{n} = n(2N_h + 1)$  unknowns ( $a_0$ ,  $a_k$ ,  $b_k$ ,  $1 \leq k \leq N_h$ ) and  $n$  denoting  $q$  size. The Galerkin approach generates the expected  $\tilde{n}$  equations by projecting this set of equations on each time dependent function used to decompose  $q(t)$  (i.e.  $1/\sqrt{2}$ ,  $\cos(k\omega t)$  and  $\sin(k\omega t)$  with  $1 \leq k \leq N_h$ ). The scalar product used is:

$$\langle f, g \rangle_T = \frac{2}{T} \int_0^T f(t)g(t)dt$$

The resulting set of equations is obviously of form (2) (details are given in appendix A).

It is interesting to note that constant solutions are a special case of  $T$ -periodic solutions when  $q(t)$  is sought as  $a_0$  only. Even if one mostly looks for cycles, it may be useful for some applications to be able to find all the fixed points solutions.

*Reduction of the problem.* Used in local search context, one often apply a Newton-Raphson scheme to these equations which means that a linear system has to be solved repeatedly: the smaller it is, the faster the solution is found. This assumption is all the more true in your case where computation cost grows severely with the system size; reducing the system can help saving hours for the resolution step. [8] proposes the exact condensation procedure that follows: let us partition the unknowns  $\tilde{x}_i$  which participate to the non-linear force expression  $\hat{H}$  and those which do not and denote  $\tilde{x}_{nl}$  the former and  $\tilde{x}_l$  the latter. Rearranging (2), one gets:

$$\begin{bmatrix} \mathbf{H}_{ll} & \mathbf{H}_{lnl} \\ \mathbf{H}_{nll} & \mathbf{H}_{nlnl} \end{bmatrix} \begin{Bmatrix} \tilde{x}_l \\ \tilde{x}_{nl} \end{Bmatrix} + \begin{Bmatrix} \hat{H}_l(\tilde{x}_{nl}) \\ \hat{H}_{nl}(\tilde{x}_{nl}) \end{Bmatrix} = \begin{Bmatrix} H_{el} \\ H_{enl} \end{Bmatrix}$$

The first rows, related to linear dofs, allow to write  $\tilde{x}_l$  as a function of  $\tilde{x}_{nl}$ :

$$\tilde{x}_l = \mathbf{H}_{ll}^{-1} \left[ H_{el} - \hat{H}(\tilde{x}_{nl}) - \mathbf{H}_{nl} \tilde{x}_{nl} \right]$$

Using this new expression, the second row set becomes a non-linear equation in  $\tilde{x}_{nl}$  of a much smaller size than (2):

$$\left( \mathbf{H}_{nlnl} - \mathbf{H}_{nll} \mathbf{H}_{ll}^{-1} \mathbf{H}_{nl} \right) \tilde{x}_{nl} + \left( \hat{H}_{nl}(\tilde{x}_{nl}) - \mathbf{H}_{nll} \mathbf{H}_{ll}^{-1} \hat{H}(\tilde{x}_{nl}) \right) = H_{enl} - \mathbf{H}_{nll} \mathbf{H}_{ll}^{-1} H_{el} \quad (3)$$

This equation is of size  $\hat{n}(2N_h + 1)$  where  $\hat{n}$  denotes the non-linear dofs number. In many cases the structure is mostly linear and contains only a few non-linear elements. This makes use of this condensation interesting in local search as well as in global search context.

### 2.2.2. From a non-linear set of equations to a polynomial one

Non-linear system (2) or (3) has now to be “converted” into a polynomial system (or algebraic system) in order to apply the final global analysis method which relies on polynomial form of the system. The method will be exposed for the non condensed formulation (2).

Many ways of doing such an approximation exist. The authors chose to use a least squares method. This simple method may not be the most adequate but is easy to implement. A comparison with different methods should be achieved, dealing not only with the error resulting from the approximation but with the shape of the polynomials used and the consequences mainly on computational cost. Whatever the method may be it has to be noticed that only the non-linear part  $\hat{H}(\tilde{x})$  has to be fitted (by  $\hat{\mathbf{P}}$ ): linear and constant parts have trivial polynomial expressions. Let us use the following notations :

a) Polynomial system  $\hat{\mathbf{P}}$  and its components  $\hat{P}_i$ :

$$\hat{\mathbf{P}}(\tilde{x}) = \begin{pmatrix} \hat{P}_1(\tilde{x}) \\ \vdots \\ \hat{P}_{\hat{n}}(\tilde{x}) \end{pmatrix}$$

b) Polynomial component  $\hat{P}_i$  as a sum of  $J_i$  coefficients and monomials products:

$$\forall i \in \{1, \dots, \hat{n}\}, \hat{P}_i(\tilde{x}_i) = \sum_{1 \leq k \leq J_i} \beta_{ik} \tilde{x}^{\alpha^{ik}},$$

$$\beta_{ik} \in \mathbb{R}, \alpha^{ik} \in \mathbb{N}^{\hat{n}}, \tilde{x}^{\alpha} = \prod_{j=1}^{\hat{n}} \tilde{x}_j^{\alpha_j}$$

c) Total degree  $d_i$  of each component:

$$d_i = \deg(\hat{P}_i) = \max_{1 \leq k \leq J_i} |\alpha^{ik}|, |\alpha^{ik}| = \sum_{j=1}^{\hat{n}} \alpha_j^{ik}$$

Using a least square method, one has to generate  $s$  points  $y^{(j)} = \hat{H}(\tilde{x}^{(j)})$  and to choose the monomials  $\tilde{x}^{\alpha^{ik}}$  that will compose each component  $\hat{P}_i$  of  $\hat{\mathbf{P}}$ . Monomials choice should be guided by the higher degree one need or can afford (see next section) to describe the true function  $\hat{H}$  and obvious properties such as parity. Once this decision is made

one finds minima of the cost functions  $\phi_i$  whose variables are coefficients  $\beta_{ik}$ ,  $1 \leq k \leq J_i$  (see Eq. (4)) by solving the linear system obtained when equating their derivatives to zero (Eq. (5) and (6)):

$$\forall i \in \{1, \dots, \tilde{n}\}, \phi_i(\beta_{i1}, \dots, \beta_{iJ_i}) = \sum_{j=1}^s \left( \hat{P}_i(\tilde{x}^{(j)}) - y^{(j)} \right)^2 \quad (4)$$

$$\forall k \in \{1, \dots, J_i\}, \frac{\partial \phi_i}{\partial \beta_{ik}} = 0 \quad (5)$$

which is equivalent to:

$$\begin{aligned} A \{\beta_{ir}\}_{1 \leq r \leq J_i} &= b \\ A_{rs} &= \sum_{j=1}^s (\tilde{x}^{(j)})^{\alpha^{ir} + \alpha^{js}}, \quad 1 \leq r, s \leq J_i \\ b_r &= \sum_{j=1}^s (\tilde{x}^{(j)})^{\alpha^{ir}} y^{(j)}, \quad 1 \leq r \leq J_i \end{aligned} \quad (6)$$

Possessing  $\hat{\mathbf{P}}$ ,  $\mathbf{P}$  which denotes the global polynomial system is obtained by simply adding the linear and constant part contributions:

$$\mathbf{P}(\tilde{x}) = \left\{ \begin{array}{c} P_1(\tilde{x}) \\ \vdots \\ P_{\tilde{n}}(\tilde{x}) \end{array} \right\}, \quad P_i(\tilde{x}) = \hat{P}_i(\tilde{x}) + \sum_{j=1}^{\tilde{n}} \mathbf{H}_{ij} \tilde{x}_j - H_{ei}, \quad 1 \leq i \leq \tilde{n} \quad (7)$$

One should notice that using the polynomial approximation is often cheaper than using the original non-linear expression obtained by HBM: HBM method requires an AFT (Alternate Frequency-Time) procedure [3] for  $\hat{H}$  term computation which is often costly enough. Using polynomials, one has to compute it  $s$  times only.

We will now focus on finding all zeros of this multivariate polynomial system.

### 2.2.3. Global resolution of the polynomial system using homotopies

Finding all the roots of a multivariate polynomial (in  $\mathbb{C}$ ) is not an easy task and one finds active research since 1977 with Garcia, Zangwill and Drexler work. More recently many papers dealt with solving multivariate polynomial systems using homotopy methods (see [25, 12, 14, 15, 29, 24] and [11] for a general overview); the reference book [21] written by Sommese and Wampler provides the full theory and great reflection about its numerical implementation.

Basically the homotopy method consists in a continuation from roots of a polynomial system  $\mathbf{Q}$  to the roots of the system at stake  $\mathbf{P}$  using the roots of the intermediate problem (8) with  $\lambda$  varying from 1 to 0:

$$\mathbf{R}(\tilde{x}, \lambda) = \lambda \mathbf{Q}(\tilde{x}) + (1 - \lambda) \mathbf{P}, \quad \lambda \in [0, 1] \quad (8)$$

Having all complex zeros of  $\mathbf{P}$ , it is easy to extract the real ones which are approximate solutions of the initial non-linear system (2).

Obviously  $\mathbf{Q}$  should have “easy-to-find” roots and it should also match some conditions to ensure that the homotopy process will provide all of  $\mathbf{P}$  zeros. First of all it should have as many zeros as  $\mathbf{P}$  because each  $\mathbf{P}$  zero must be linked to a  $\mathbf{Q}$  zero through a continuous path. Then, it must share structural properties with  $\mathbf{P}$  so as to avoid bifurcation

along continuation (which would make the whole procedure inefficient). A simple  $\mathbf{Q}$  that respects these conditions and has easy to find roots is:

$$\mathbf{Q}(\tilde{x}) = \gamma \left\{ \begin{array}{c} \tilde{x}_1^{d_1} - 1 \\ \vdots \\ \tilde{x}_n^{d_n} - 1 \end{array} \right\}, \quad \gamma \in \mathbb{C}, \quad d_i = \deg(P_i) \quad (9)$$

A total-degree-homotopy theorem ([21, Chap. 8, p. 123]) ensures that following all  $\mathbf{Q}$  roots, one will find all the nonsingular solutions of  $\mathbf{P}(\tilde{x}) = 0$  (solved in  $\mathbb{C}^{\tilde{n}}$ ). The problem is that most of the  $\mathcal{N} = \prod_{i=1}^{\tilde{n}} d_i$  paths followed will not converge to a sought solution but diverge to infinity and so, are worthless to follow. If dealing with divergence is no real problem (solved using a homogeneization technique explained below), following a huge number of paths can make this method become unusable practically. That is why most of the papers deal with building initial polynomial sets  $\mathbf{Q}$  that have the fewest roots while still having easy to find ones.

Among these methods are the total degree homotopy method and the multihomogeneous homotopy method (often referred to as  $m$ -homogeneous homotopy). The first one consists in using a polynomial  $\mathbf{Q}$  as expressed in (9) considering that all variables  $\tilde{x}_i$  play the same role: no real analysis of  $\mathbf{P}$  is required but it generates the maximum number of paths (majored by Bézout number  $\mathcal{N}$ ). The second one uses  $m$  groups of variables taking into account, for example, that most of them only have a linear contribution while a few have a non-linear (high degree) contribution. The number of paths generated using such a method is given by the Bézout theorem adapted to multi-homogeneous structures [21]; optimal partitioning methods can be found in [23, 13, 22].

To better understand the difference between these two methods, one needs to describe what homogeneization means. The shortest way to explain it is: turning each monomial with degree  $d_i$  of a polynomial with total degree  $d = \max d_i$  into monomials with the same degree  $d$  by multiplying them by  $\tilde{x}_0^{(d-d_i)}$  where  $\tilde{x}_0$  is a homogeneization variable. Then

$$\forall (\tilde{x}_0, \tilde{x}_1, \dots, \tilde{x}_n) \in \mathbb{C}^{(P+1)}, \quad \forall \mu \neq 0, \quad \mathbf{P}(\mu(\tilde{x}_0, \tilde{x}_1, \dots, \tilde{x}_n)) = \mu^d \mathbf{P}(\tilde{x}_0, \tilde{x}_1, \dots, \tilde{x}_n)$$

which is at least an interesting property for dealing with divergence: if  $\mathbf{P}(\tilde{x}_1, \dots, \tilde{x}_n)$  is the polynomial system to solve, let's denote  $\mathbf{P}_h(\tilde{x}_0, \tilde{x}_1, \dots, \tilde{x}_n)$  the equivalent system where each  $P_k$  component is homogeneized. Adding an unknown  $\tilde{x}_0$ , one needs to add an equation; for example,

$$\max_{0 \leq i \leq P} |\tilde{x}_i| = 1$$

This leads to a homogeneized continuation system  $\mathbf{R}_h((\tilde{x}_0, \dots, \tilde{x}_n), \lambda) = 0$ . If during continuation, one of the  $\tilde{x}_i$  become huge to satisfy  $\mathbf{R}_h((\tilde{x}_0, \dots, \tilde{x}_n), \lambda) = 0$ , one can use  $\mu = 1/|\tilde{x}_i|$  and rewrite:

$$\mathbf{R}_h(\mu(\tilde{x}_0, \dots, \tilde{x}_n), \lambda) = \mu^d \mathbf{R}_h((\tilde{x}_0, \dots, \tilde{x}_n), \lambda) = 0$$

$\mu(\tilde{x}_0, \dots, \tilde{x}_n)$  is not that huge anymore and still satisfies the continuation equation. Plus, solutions obtained when  $\lambda$  tends towards 0 whose  $\tilde{x}_0$  component tends towards 0 are points to infinity.

Generalizing this, one can use more than one homogeneization variable. For example  $m$  variables denoted  $\tilde{z}_1, \dots, \tilde{z}_m$ .

If generalized unknowns are partitioned in  $m$  groups  $Z_k = \{\tilde{x}_i, i \in \mathcal{K}_k\}$ , with  $\cup_{1 \leq k \leq m} \mathcal{K}_k = \{1, \dots, \tilde{n}\}$  and  $\forall 1 \leq i < j \leq m, \mathcal{K}_i \cap \mathcal{K}_j = \emptyset$ , a homogeneization variable  $\tilde{z}_k$  can be affected to each group of generalized unknowns  $Z_k$ . A degree table  $D = (d_{ij})_{1 \leq i \leq \tilde{n}, 1 \leq j \leq m}$  can then be established with  $d_{ij}$  denoting the maximum degree of group  $\mathcal{K}_j$  variables observed in monomials of  $P_i$ . Then, for each  $P_i$  component of  $\mathbf{P}$  a multi-homogeneization step can be achieved by bringing each  $P_i$  monomial to the same degree  $\sum_j d_{ij}$  using the  $m$  homogeneization variables: each generalized unknown  $\tilde{x}_i$  in group  $Z_k$  is temporarily replaced by  $\tilde{x}_i/\tilde{z}_k$  and the resulting denominators are cleared by multiplying  $P_i$  by  $\prod_{1 \leq k \leq m} \tilde{z}_k^{d_{ik}}$ . The multi-homogenized polynomial  $\mathbf{P}_h(\tilde{z}_1, \dots, \tilde{z}_m, \tilde{x}_1, \dots, \tilde{x}_{\tilde{n}})$  has then component  $P_{hi}$  whose monomials share the same degree  $\sum_j d_{ij}$  but where generalized unknowns of different groups are treated differently. This approach is interesting whenever some variables occur with low degrees only (generalized unknowns related to linear dofs) and a few of them occur with high degrees (generalized unknowns related to non-linear dofs). an initial polynomial  $\mathbf{Q}$  as specified in (10) (the important point is that  $\mathbf{P}$  and  $\mathbf{Q}$  have the same degree table  $D$ ) can then be used and has easy to find roots.

$$\mathbf{Q}(\tilde{x}) = \gamma \left\{ \begin{array}{c} (\tilde{x}_{\mathcal{K}_1}^{d_{11}} - 1) \times \dots \times (\tilde{x}_{\mathcal{K}_m}^{d_{1m}} - 1) \\ \vdots \\ (\tilde{x}_{\mathcal{K}_1}^{d_{\tilde{n}1}} - 1) \times \dots \times (\tilde{x}_{\mathcal{K}_m}^{d_{\tilde{n}m}} - 1) \end{array} \right\}, \gamma \in \mathbb{C} \quad (10)$$

where  $\tilde{x}_{\mathcal{K}_i}$  stands for one of the generalized unknowns in group  $\mathcal{K}_i$ .

These homotopy methods have a great advantage over cell-exclusion or interval analysis based ones: they allow computational time estimation. Knowing in advance the number of paths to be followed, it is easy to compute a few of them, obtaining then a rough estimation for the whole stack. Plus, they do not require to be given an arbitrary initial bounded space where to look for the solutions whereas the three others do: they ensure to get all the solutions, letting us decide *a posteriori* if they have a physical meaning or interest, or not.

### 3. Comparison with other global analysis methods on a simple Duffing oscillator

In order to evaluate the efficiency of the proposed approach, it will be compared to three different methods using a classical non-linear Duffing oscillator. The results exposed come from the PhD Thesis [18] where details can be found.

The forced Duffing oscillator at stake is :

$$\ddot{q} + 2\xi\omega_0\dot{q} + \omega_0^2q + \beta q^3 = \Gamma \cos(\omega t) \quad (11)$$

with numerical values  $\xi = 0.02$ ,  $\omega_0 = 1 \text{ rad.s}^{-1}$ ,  $\beta = 1 \text{ s}^{-2}$  and  $\Gamma = 0.1 \text{ m.s}^{-2}$ . This forced oscillator has the frequency response given in figure 4; this curve is obtained using a continuation method. While looking for multiple solution sets, global analysis methods are applied for  $\omega = 1.2 \text{ rad.s}^{-1}$  : three solutions - two stable  $S_1$  and  $S_3$  and one unstable  $S_2$  - coexist as shown on the figure.

[Figure 4 about here.]

The main characteristics of used methods are given below:

- (a) simple cell-mapping: bounded state space portion  $(q, \dot{q})$  considered is  $[-2, 2] \times [-3, 3]$  using 100 divisions in each directions (leading to 10 000 cells to be examined). Each cell center is a startpoint for a time-integration scheme with duration  $\tau = 2\pi/\omega$ .
- (b) exclusion test method: dynamic equation (11) is turned into a non-linear system using HBM with different harmonic numbers  $N_h$  in order to obtain different sizes for the problem (2). The exclusion test used is based on simplex method [27]. Each  $\tilde{x}_i$  unknown is sought in a bounded box equal to  $[-2, 2]$ .
- (c) interval analysis method: dynamic equation (11) is turned into a non-linear set using HBM with different harmonic numbers  $N_h$  in order to obtain different sizes for the problem (2). The algorithm used is based on the one proposed by Hansen and Walster in [9]; a matlab toolbox, Intlab, provided by the Institute for Reliable Computing (<http://www.ti3.tu-harburg.de/>) is used to deal with intervals. Each  $\tilde{x}_i$  unknown is sought in an interval equal to  $[-2, 2]$ .
- (d) polynomial homotopy method: dynamic equation (11) is turned into a non-linear set using HBM with different harmonic numbers  $N_h$  in order to obtain different sizes for the problem (2). This problem is already polynomial (total degree 3): no polynomial approximation step is performed. A total degree homotopy method is used to build the initial polynomial  $\mathbf{Q}$ .

Every method is implemented by using Matlab 7; the calculations are made on a Core 2 Duo E6600 (4Go RAM).

[Figure 5 about here.]

First, methods are applied to the Duffing oscillator, with various harmonic decompositions for methods (b) to (d) in order to get some reference times. Then, extrapolations are computed to investigate the methods efficiency for larger systems. Figure 5 summarizes the results. As cell-mapping is applied directly on the dynamic equation while other methods are applied to the transformed non-linear set of equations, results are not exposed the same way. The first graphic deals with the simple cell-mapping method. It shows the computation time required to process systems of 1 to 3 dofs using 10, 20, 30, 40, 50 or 100 divisions in each direction of the investigated bounded portion of the state space. The second graphic gives the time required for systems with up to 10  $\tilde{x}_i$  unknowns (with a degree 3 polynomial approximation and an initial polynomial based on total degree in case of method (d)). The number of dofs related to this number of generalized unknowns depends on the harmonic decomposition used: 5 dofs using only 1 harmonic (no constant) leads to 10 generalized unknowns as do 2 dofs with a constant term and 2 harmonics. Axis of ordinate is logarithmic and representative time units are indicated. This shows that the proposed method is obviously faster than methods (b) and (c); for comparison with method (a), one can consider a 2 dofs system with a constant term and 2 harmonics decomposition (10  $\tilde{x}_i$  unknowns): the cell-mapping with 50 divisions in each direction and the polynomial homotopy method seem then cost equivalent. Drawbacks of the cell-mapping method is the need of a bounded state

space where solutions are sought and the arbitrary number of divisions used: with only 50 divisions, one may be brought to refine some areas of interest and so to increase the time required to get the solutions. Furthermore, required time growth with system size is much bigger for the cell-mapping than for the polynomial homotopy method. Finally, the proposed approach can be easily parallelized as each path can be followed independently.

According to its efficiency and potential, one proposes to evaluate this most promising technique on a some more complex example.

#### 4. Application to a squeeze-film supported rotor

We will now apply homotopy methods to a simple model of rotor damped using a squeeze-film bearing (fig. 6).

[Figure 6 about here.]

This system has already been studied in [28] using local methods. It consists in a stiff and damped rotor  $m_1, c_1, k_1$  (including rolling bearing and squeeze-film inner ring) mounted on a squeeze-film bearing with outer ring  $m_2$  linked to the “basement” through  $c_2, k_2$ ; excitation comes from the unbalance  $U$ . Dynamic equations are (12) (using notations of appendix B) where the non-linearity is induced by the squeeze-film through  $F_x$  and  $F_y$  efforts:

$$\mathbf{M}\ddot{q} + \mathbf{C}\dot{q} + \mathbf{K}q + \begin{pmatrix} -F_x \\ -F_y \\ F_x \\ F_y \end{pmatrix} = \begin{pmatrix} U \cos \tau \\ U \sin \tau \\ 0 \\ 0 \end{pmatrix} \quad (12)$$

##### 4.1. From dynamic to non-linear equations

Using the classical centered circular synchronous orbiting assumption for the rotor and a concentric movement assumption for the whole system, one can simplify the equations by rewriting  $q$  and the non-linear efforts  $F_x$  and  $F_y$ :

$$q(t) = \begin{pmatrix} a_1 \\ b_1 \\ a_2 \\ b_2 \end{pmatrix} \cos \tau + \begin{pmatrix} b_1 \\ -a_1 \\ b_2 \\ -a_2 \end{pmatrix} \sin \tau \quad (13)$$

$$F_r = \left(-\frac{B}{s}\right) \left(2 \frac{\epsilon^2}{(1-\epsilon^2)^2} \omega\right) \quad (14)$$

$$F_t = \left(-\frac{B}{s}\right) \left(\frac{\pi}{2} \frac{\epsilon}{(1-\epsilon^2)^{3/2}} \omega\right) \quad (15)$$

As harmonic coefficients in  $\cos \tau$  and  $\sin \tau$  are bound because of circular orbiting assumption, one only needs to solve equations obtained by balancing (12) with respect to  $\cos \tau$ :

$$\underbrace{\left( \mathbf{K} - \mathbf{M} + \mathbf{C} \begin{bmatrix} 0 & -1 \\ 1 & 0 & & \\ & & 0 & -1 \\ & & & 1 & 0 \end{bmatrix} \right)}_{\mathbf{H}} \tilde{x} + \underbrace{\begin{bmatrix} -H_x \\ -H_y \\ H_x \\ H_y \end{bmatrix}}_{\hat{H}(\tilde{x})} = \underbrace{\begin{bmatrix} U \\ 0 \\ 0 \\ 0 \end{bmatrix}}_{H_e}, \quad H_{x/y}(\tilde{x}) = \frac{1}{\pi} \int_0^{2\pi} F_{x/y}(\tilde{x}) \cos(\tau) d\tau \quad (16)$$

#### 4.2. Building the polynomial approximation

We now need to build a polynomial approximation  $\hat{\mathbf{P}}(\tilde{x})$  of the non-linear part  $\hat{H}(\tilde{x})$ . First let us notice that it depends only on  $\epsilon$  that is the relative displacements  $X_2 - X_1$  and  $Y_2 - Y_1$ : the change of variables (17) is applied.

$$q = \mathcal{B}q_r, \quad \mathcal{B} = \begin{bmatrix} 1 & & & \\ & 1 & & \\ 1 & & 1 & \\ & & & 1 & 1 \end{bmatrix} \quad (17)$$

From now on  $\tilde{x}$  will denote harmonics vector of  $q_r$  decomposition:

$$q_r = \underbrace{\begin{bmatrix} a_1 \\ b_1 \\ a_r \\ b_r \end{bmatrix}}_{\tilde{x}} \cos \tau + \begin{bmatrix} b_1 \\ -a_1 \\ b_r \\ -a_r \end{bmatrix} \sin \tau \quad (18)$$

This change of variables has small changes on (16) but allows us to use a 2 variables polynomial (whose variables are  $a_r$  and  $b_r$ ) instead of a 4 variables one which saves monomials used to express the polynomial and so computation time required to evaluate it and even more, as we will see in the next subsection when applying a homotopy method.

[Figure 7 about here.]

As mentioned in section 2.2.2, a least squares method is used to fit  $\hat{H}$ . Two polynomial approximations are built: one using degree 6 polynomials and the other using degree 12 polynomials. The choice is made to generate points  $y^{(j)}$  used for fitting that respect  $0 \leq \epsilon \leq 0.6$ ; that is,  $a_r$  and  $b_r$  couples are picked up such that  $0 \leq \sqrt{a_r^2 + b_r^2} \leq 0.6$ . This is motivated by the physical reality: formulas used to approximate squeeze-film efforts are not valid beyond such eccentricities.

Figure 7 allows some qualitative comparison between the true values of  $H_x$  and the ones obtained using polynomial approximations while figure 8 gives quantitative results for degree 12 approximation of  $H_x$ : mean relative error is plotted for small rings along  $\epsilon$  and shows good agreement with the original function with less than 5% error for

almost all  $\epsilon$  between 0.2 and 0.6. Bad results obtained for very small  $\epsilon$  values can be explained by almost zero value of  $H_x$  for small eccentricities - such eccentricities are not of great interest anyway because non-linear effects are then almost negligible.

[Figure 8 about here.]

Polynomial systems obtained after fitting are augmented with linear and excitation parts  $\mathbf{H}$  and  $H_e$  to obtain  $\mathbf{P}(\tilde{x})$  as defined in sec. 2.2.2.

#### 4.3. Global analysis using homotopies

Different homotopy methods were tested for one configuration ( $s = 1$ ) and for each polynomial approximation degree  $d$  ( $d = 6$  or  $d = 12$ ):

- (a) Total degree homotopy on full system: the  $\tilde{n} = 4$  generalized unknowns are kept and considered the same way. Each of the four equations  $\mathbf{P}_i(\tilde{x})$  is of degree 6 or 12, leading to  $d^4$  paths to follow.
- (b) 2-homogeneous homotopy on full system: the 4 unknowns are partitioned into 2 subsets; one of them contains linear variables  $a_1$  and  $b_1$  and the other contains non-linear ones  $a_r$  and  $b_r$ . The number of paths to continue is then  $6d^2$ .
- (c) Total degree homotopy on reduced system: after applying the exact condensation of section 2.2.1, a new polynomial system is computed (containing the only 2 non-linear variables  $a_r$  and  $b_r$ ) and a total degree homotopy method is applied, generating  $d^2$  paths.

The results in terms of number of paths and time required to obtain the complex solutions are summed up in table 1.

[Table 1 about here.]

Every method ends in a reasonable amount of time but there exists a great gap between each of them, the best being the total degree homotopy used to solve the condensed system.

This method was then used with degree 12 approximation for several  $s$  values. The real solutions - the only ones of interest - are kept and plotted using red points on figure 9.

[Figure 9 about here.]

The solid blue and dashed green curves were obtained using a continuation scheme (see [2] for details). The solid (lower) one is the classical dynamic response obtained when using a continuation scheme starting from a local search for a small  $s$  value. The dashed (upper) one is the curve obtained after a local search using one of the global analysis results as a startpoint. The gap between the second branch depicted by global analysis points and the one obtained using a local continuation scheme results from the error made by the polynomial approximation for large eccentricities.

This shows how important it is to possess a global analysis tool: without it, one would not look for an another branch of solutions, disconnected from the solid one, appearing without any obvious bifurcation.

A stability study is conducted for these two branches using Floquet theory (figure 10): the second branch has stable solutions of large eccentricities coexisting with solutions of the classical one. Figure 11 shows that the second branch, on its stable part, consists in orbits of quite the same magnitude than orbits of the first branch for the rotor, but squeeze-film orbits are much greater; in fact, the squeeze-film outer-ring orbits outside the journal orbit.

[Figure 10 about here.]

[Figure 11 about here.]

One already mentioned that the  $\pi$ -film model was not a good one to describe such large eccentricities so squeeze-film damper users should not be afraid of this new branch until other tests using proper models are done. Nevertheless, this points out the need to be careful when working with such great eccentricities, and shows the ability of the method to exhibit unexpected disconnected branches of solutions, which was at stake.

## 5. Conclusion

This paper exposes a global analysis method able to find all the  $T$ -periodic solutions of a dynamical non-linear system. It is based on three major steps: first a harmonic balance to transform dynamic equations into a non-linear non-differential system; this system is then put into a polynomial form in order to proceed to the global analysis (finding all its roots) using a homotopy technique. It has been shown to be the most efficient approach when compared to three other global analysis methods applied to a Duffing oscillator.

A simple model of rotor supported by a squeeze-film damper emphasizes then the ability of the method to find disconnected solutions and its computational efficiency. High degree polynomial approximations of non-linear part can be treated in a reasonable amount of time which allows to treat complex non-linearity expressions.

The harmonic balance was applied using a known period  $T$ ; further work will be achieved so as to let it free, by adding for example a phase equation [19]. Another interesting improvement will be to compare different polynomial approximation methods linked with variables space partitioning to save computational time. Finally, parallelization could be easily implemented as each path of the homotopy step can be processed independently which would help to save a lot of computation time.

### A. HBM elements definition

a) Vector of generalized unknowns  $\tilde{x}$ :  $\tilde{x} = \{a_0, a_1, b_1, \dots, a_{N_h}, b_{N_h}\}^t \in \mathbb{R}^{t(2N_h+1)}$

Displacement  $q(t)$  is a function of  $\tilde{x}$ :  $q(t) = \phi_\omega(\tilde{x}) = \frac{a_0}{\sqrt{2}} + \sum_{k=1}^{N_h} a_k \cos(k\omega t) + b_k \sin(k\omega t)$

b) Linear part  $\mathbf{H}\tilde{x}$ :

$$\mathbf{H} = \begin{bmatrix} \Lambda_0 & & & \\ & \Lambda_1 & & \\ & & \ddots & \\ & & & \Lambda_{N_h} \end{bmatrix}, \text{ with } \begin{cases} \Lambda_0 = \mathbf{K} \in \mathcal{M}_N(\mathbb{R}) \\ \Lambda_k = \begin{bmatrix} \mathbf{K} - (k\omega)^2\mathbf{M} & -(k\omega)\mathbf{C} \\ (k\omega)\mathbf{C} & \mathbf{K} - (k\omega)^2\mathbf{M} \end{bmatrix}, \Lambda_k \in \mathcal{M}_{2N}(\mathbb{R}), 1 \leq k \leq N_h \end{cases}$$

c) Non-linear part  $\hat{H}(\tilde{x})$  and constant term  $H_e$ :

$$\hat{H}(\tilde{x}) = \begin{cases} \langle \hat{f}(\phi_\omega(\tilde{x})), 1/\sqrt{2} \rangle_T \\ \vdots \\ \langle \hat{f}(\phi_\omega(\tilde{x})), \cos(k\omega t) \rangle_T \\ \langle \hat{f}(\phi_\omega(\tilde{x})), \sin(k\omega t) \rangle_T \\ \vdots \end{cases}_{1 \leq k \leq N_h}, H_e = \begin{cases} \langle f_e(t), 1/\sqrt{2} \rangle_T \\ \vdots \\ \langle f_e(t), \cos(k\omega t) \rangle_T \\ \langle f_e(t), \sin(k\omega t) \rangle_T \\ \vdots \end{cases}_{1 \leq k \leq N_h}$$

## B. Squeeze-film example notations

### B.1. Initial system of equations

$$\begin{cases} m_1 x_1'' + c_1 x_1' + k_1 x_1 = f_x + m_1 u \omega^2 \cos(\omega t) \\ m_1 y_1'' + c_1 y_1' + k_1 y_1 = f_y + m_1 u \omega^2 \sin(\omega t) \\ m_2 x_2'' + c_2 x_2' + k_2 x_2 = -f_x \\ m_2 y_2'' + c_2 y_2' + k_2 y_2 = -f_y \end{cases}, \text{ with } z' = \frac{\partial z}{\partial t}, \text{ leads to (12) after division by } m_1 C \omega^2.$$

### B.2. Dimensionless variables

$$\tau = \omega t, \dot{z} = \partial z / \partial \tau, s = \omega / \omega_1, \alpha = m_2 / m_1, \beta = k_2 / k_1, \xi_1 = c_1 / (m_1 \omega_1), \xi_2 = c_2 / (m_2 \omega_2), \\ X_i = x_i / C, Y_i = y_i / C, U = u / C, F_x = f_x / (m_1 C \omega^2), q = \{X_1, Y_1, X_2, Y_2\}^t, \epsilon = \sqrt{(X_1 - X_2)^2 + (Y_1 - Y_2)^2}$$

### B.3. Matrices

$$\mathbf{M} = \text{diag}(1, 1, \alpha, \alpha), \mathbf{C} = \frac{1}{s} \text{diag}(\xi_1, \xi_1, \xi_2 \sqrt{\alpha\beta}, \xi_2 \sqrt{\alpha\beta}), \mathbf{K} = \frac{1}{s^2} \text{diag}(1, 1, \beta, \beta)$$

### B.4. SF contribution using a short bearing approximation and a $\pi$ -film cavitation model

$$F_r = \left(-\frac{B}{s}\right) \left[ \frac{\pi}{2} \frac{1 + 2\epsilon^2}{(1 - \epsilon^2)^{5/2}} \dot{\epsilon} + 2 \frac{\epsilon^2}{(1 - \epsilon^2)^2} \dot{\phi} \right], F_t = \left(-\frac{B}{s}\right) \left[ 2 \frac{\epsilon}{(1 - \epsilon^2)^2} \dot{\epsilon} + \frac{\pi}{2} \frac{\epsilon}{(1 - \epsilon^2)^{3/2}} \dot{\phi} \right], \\ F_x = F_t \cos \phi + F_r \sin \phi, F_y = -F_r \cos \phi + F_t \sin \phi$$

### B.5. Numerical values

$$B = 0.1, U = 0.4, \xi_1 = 0, \xi_2 = 0.05, \alpha = 0.05, \beta = 1$$

## References

- [1] G. Alefeld and G. Mayer. Interval analysis: theory and applications. *Journal of Computational and Applied Mathematics*, 121(1):421–464, 2000.
- [2] E. L. Allgower and K. Georg. *Introduction to Numerical Continuation Methods*. Springer-Verlag, 2003.
- [3] T. M. Cameron and J. H. Griffin. An alternating frequency/time domain method for calculating the steady-state response of nonlinear dynamic systems. *Journal of Applied Mechanics*, 56(1):149–154, 1989.
- [4] Q. Ding, J.E. Cooper, and A.Y.T. Leung. Application of an improved cell mapping method to bilinear stiffness aeroelastic systems. *Journal of Fluids and Structures*, 20(1):35–49, 2005.
- [5] K. Georg. Improving the efficiency of exclusion algorithms. *Advances in Geometry*, 1:193–210, 2001.
- [6] K. Georg. A new exclusion test. *Journal of Computational and Applied Mathematics*, 152:147–160, 2003.
- [7] R. Guder and E. Kreuzer. Control of an adaptive refinement technique of generalized cell mapping by system dynamics. *Nonlinear Dynamics*, 20(1):2132, 1999.
- [8] E. J. Hahn and P. Y. P. Chen. Harmonic balance analysis of general squeeze film damped multidegree-of-freedom rotor bearing systems. *Journal of Tribology*, 116(3):499–507, 1994.
- [9] E. Hansen and G. W. Walster. *Global Optimization Using Interval Analysis*. M. Dekker, 2004.
- [10] C.S. Hsu. *Cell-to-Cell Mapping, a method of global analysis for non linear systems*. Springer-Verlag, 1987.
- [11] T. Y. Li. Numerical solution of multivariate polynomial systems by homotopy continuation methods. *Acta Numerica*, 6:399–436, 1997.
- [12] T. Y. Li, T. Sauer, and J. A. Yorke. The random product homotopy and deficient polynomial systems. *Numerische Mathematik*, 51(5): 481–500, 1987.
- [13] Heng Liang, Fengshan Bai, and Leyuan Shi. Computing the optimal partition of variables in multi-homogeneous homotopy methods. *Applied Mathematics and Computation*, 163(2):825–840, April 2005.
- [14] A. Morgan and A. Sommese. A homotopy for solving general polynomial systems that respects m-homogeneous structures. *Applied Mathematics and Computation*, 24(2):101–113, 1987.
- [15] A. Morgan and A. Sommese. Computing all solutions to polynomial systems using homotopy continuation. *Applied Mathematics and Computation*, 24(2):115–38, 1987.
- [16] S. Nacivet, C. Pierre, F. Thouverez, and L. Jezequel. A dynamic lagrangian frequency-time method for the vibration of dry-friction-damped systems. *Journal of Sound and Vibration*, 265(1):201 – 219, 2003.
- [17] A. H. Nayfeh and B. Balachandran. *Applied Nonlinear Dynamics*. Wiley Series in Nonlinear Science, 1995.
- [18] Emmanuelle Sarrouy. *Analyse globale de systmes mcaniques non-linaires - Application la dynamique des rotors*. PhD thesis, École Centrale de Lyon, October 2008. URL <http://tel.archives-ouvertes.fr/tel-00366857/fr/>.
- [19] R. Seydel. *From Equilibrium to Chaos, Practical Bifurcation and Stability Analysis*. Elsevier, 1988.
- [20] J. J. Sinou, F. Thouverez, and L. Jezequel. Center manifold and multivariable approximants applied to non-linear stability analysis. *International Journal of Non-Linear Mechanics*, 38(9):1421 – 1442, 2003.
- [21] A. J. Sommese and C. W. Wampler. *The Numerical Solution of Systems of Polynomials Arising in Engineering and Science*. World Scientific Publishing Co. Pte. Ltd., 2005.
- [22] Yuhui Tao, Heng Liang, and Fengshan Bai. A hybrid algorithm for multi-homogeneous bzout number. *Applied Mathematics and Computation*, 189(2):1755–1764, June 2007.
- [23] C. W. Wampler. Bézout number calculations for multi-homogeneous polynomial systems. *Applied Mathematics and Computation*, 157(2-3): 143–157, 1992.
- [24] L. T. Watson. Probabilility-one homotopies in computational science. *Journal of Computational and Applied Mathematics*, 140(1-2):785–807, 2002.
- [25] A. H. Wright. Finding all solutions to a system of polynomial equations. *Mathematics of Computation*, 44(169):125–133, 1985.

- [26] Z-B. Xu, J-S. Zhang, and W. Wang. A cell exclusion algorithm for determining all the solutions of a nonlinear system of equations. *Applied Mathematics and Computation*, 80:181–208, 1996.
- [27] K. Yamamura, P. Kawata, and A. Tokue. Interval solution of nonlinear equations using linear programming. *BIT*, 38(1):186–199, 1998.
- [28] J. Y. Zhao and E. J. Hahn. Eccentric operation and blade-loss simulation of a rigid rotor supported by an improved squeeze film damper. *Journal of Tribology*, 117:490–497, 1995.
- [29] W. Zulehner. A simple homotopy method for determining all isolated solutions to polynomial systems. *Mathematics of Computation*, 50(181):167–177, 1988.

## List of Figures

1	Simple cell-mapping example	19
2	Exclusion test methods: General algorithm	20
3	Interval analysis methods: General algorithm	21
4	Forced Duffing oscillator: (a) Oscillator plan, (b) Frequency response	22
5	Global analysis methods comparison	23
6	Squeeze-film supported rotor: model	24
7	Polynomial approximations of $H_x$	25
8	Degree 12 approximation of $H_x$ : mean relative error per ring	26
9	A new branch of solutions	27
10	Stability study for both branches	28
11	Squeeze-film: time integrations	29

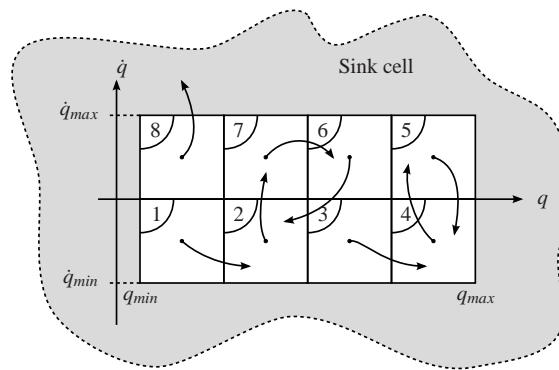


Figure 1: Simple cell-mapping example

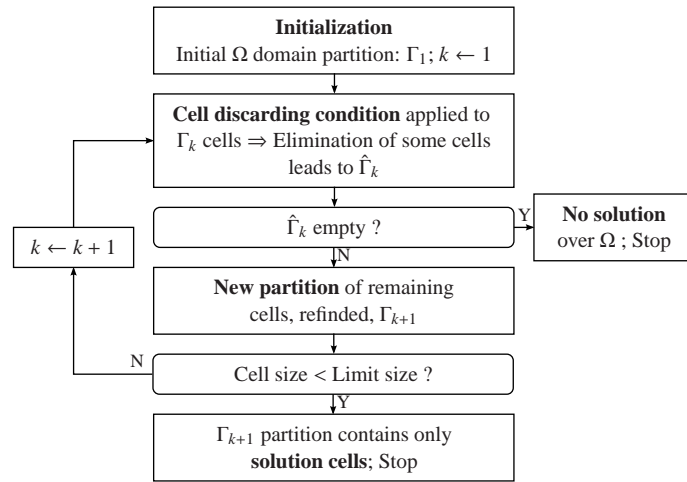


Figure 2: Exclusion test methods: General algorithm

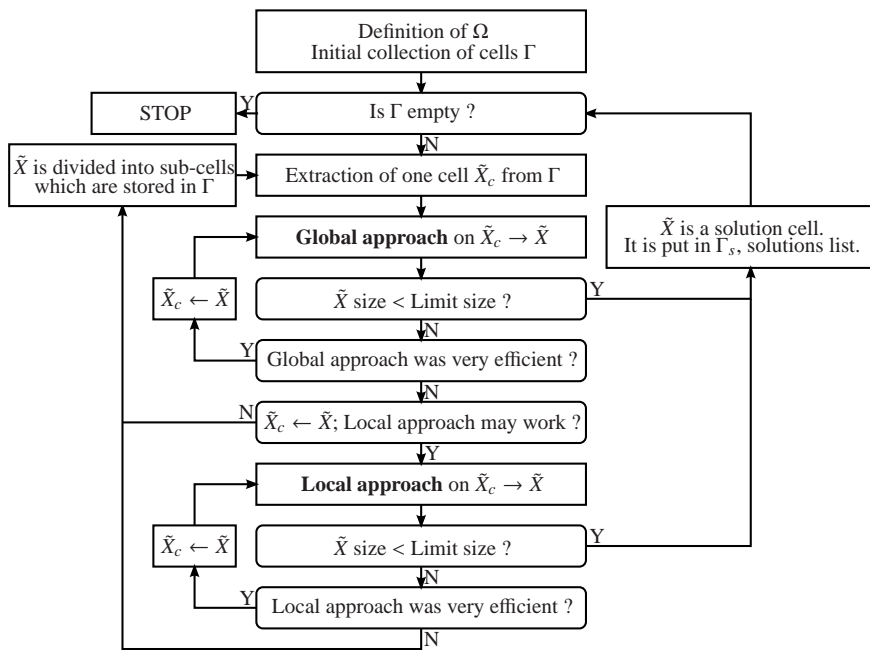


Figure 3: Interval analysis methods: General algorithm

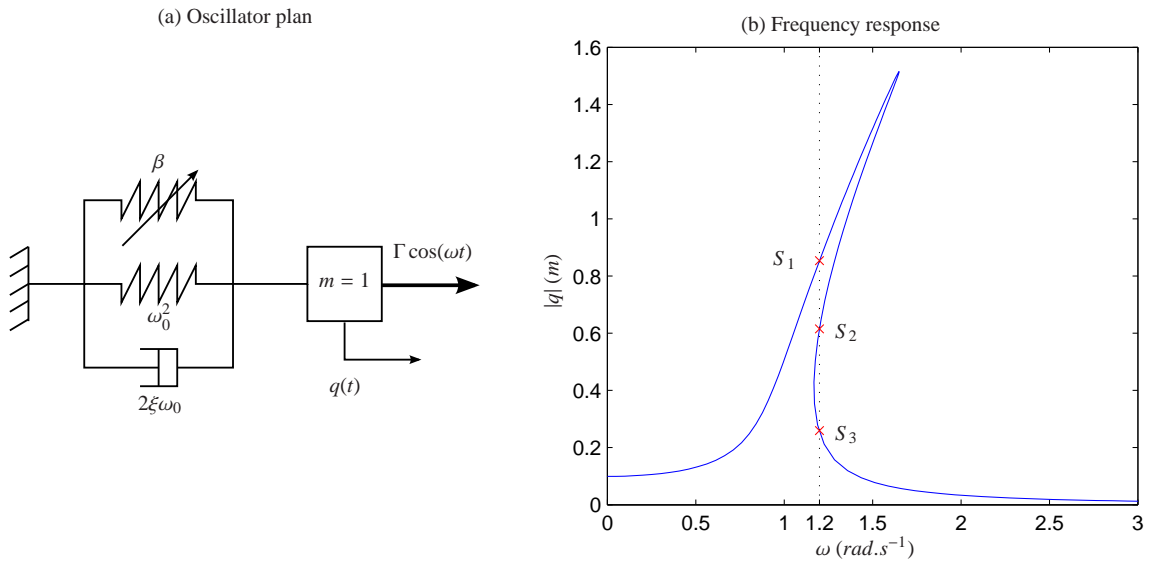


Figure 4: Forced Duffing oscillator: (a) Oscillator plan, (b) Frequency response

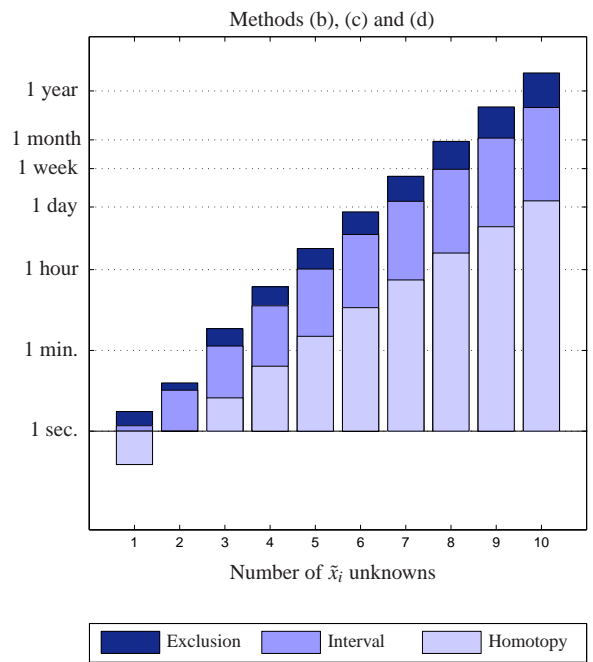
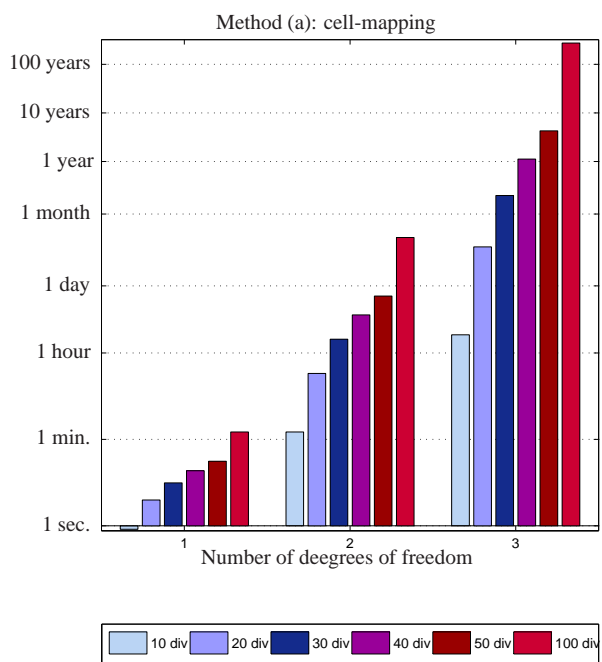


Figure 5: Global analysis methods comparison

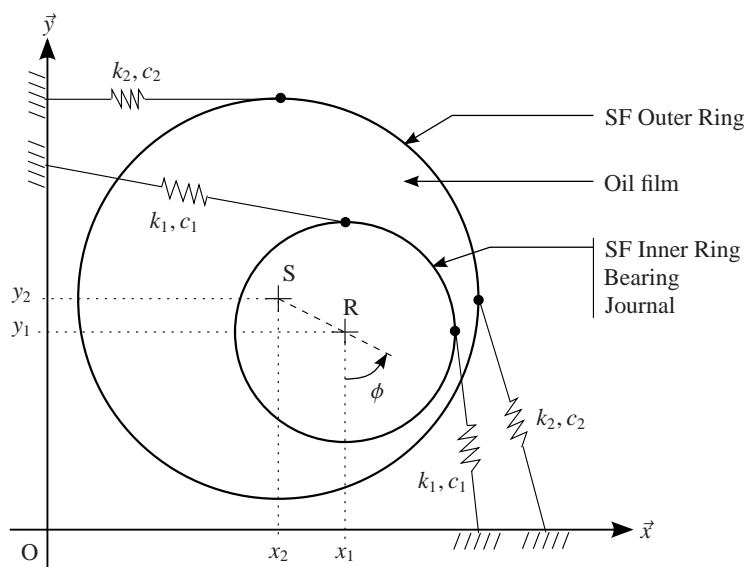
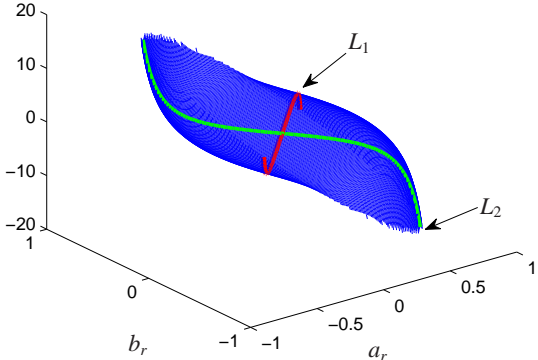
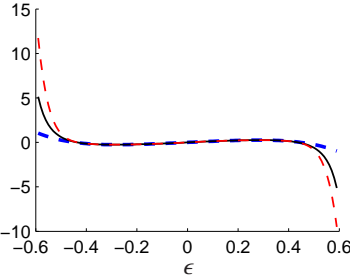


Figure 6: Squeeze-film supported rotor: model

(a) Real  $H_x$  response surface



(b)  $L_1$  cut



(c)  $L_2$  cut

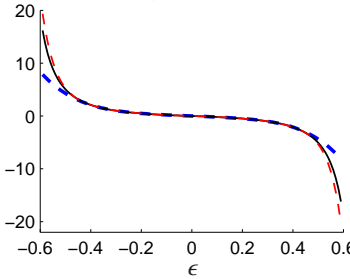


Figure 7: Polynomial approximations of  $H_x$

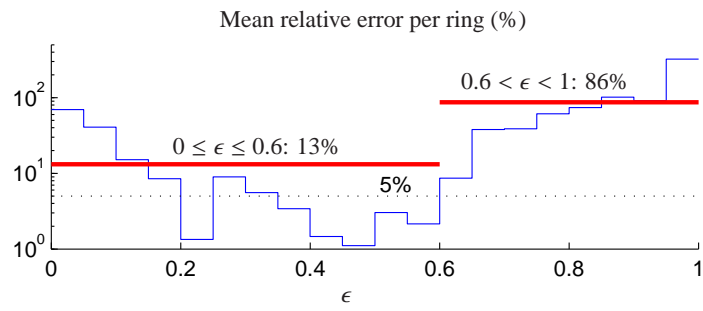


Figure 8: Degree 12 approximation of  $H_x$ : mean relative error per ring

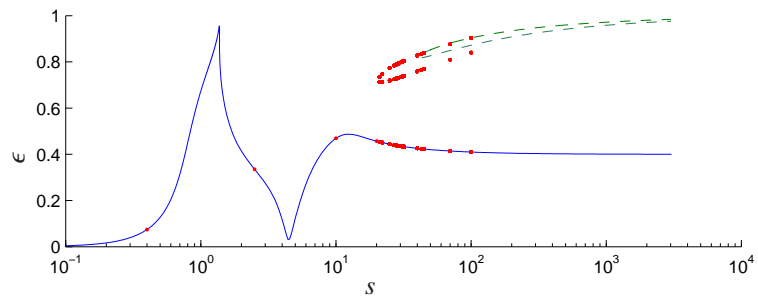


Figure 9: A new branch of solutions \* —: classical branch (branch 1) obtained using a continuation scheme starting from a local search solution point, - - : new branch (branch 2) obtained using a continuation scheme starting from global analysis solution point, • : global analysis solution points

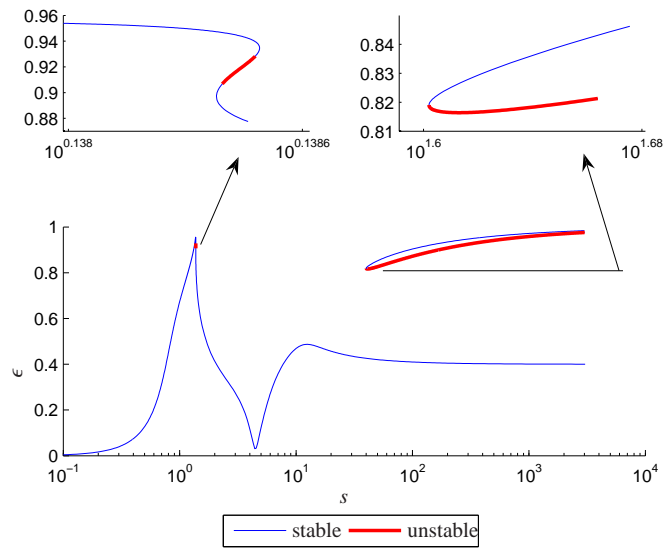


Figure 10: Stability study for both branches

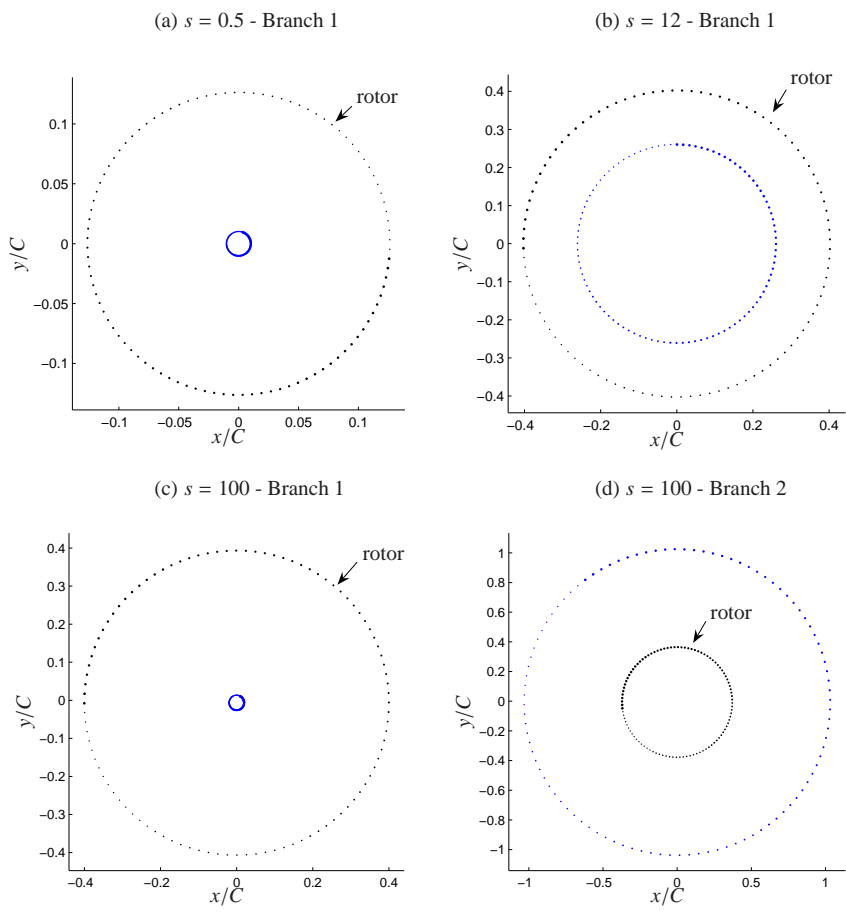


Figure 11: Squeeze-film: time integrations \* •: rotor center, •: squeeze-film center - Dots become bigger as time increases.

**List of Tables**

1 Numerical cost for different homotopy methods . . . . . 31

	Deg 6		Deg 12	
	# Paths	Time	# Paths	Time
(a) Total - Full	1296	7 min	20736	4 h
(b) 2-hom - Full	216	69 s	864	10 min
(c) Total - Red	36	4 s	144	36 s

Table 1: Numerical cost for different homotopy methods